Multitude of Core-Localized Shear Alfvén Waves in a High-Temperature Fusion Plasma

R. Nazikian,[1,*] H. L. Berk,[2] R. V. Budny,[1] K. H. Burrell,[3] E. J. Doyle,[4] R. J. Fonck,[5] N. N. Gorelenkov,[1] C. Holcomb,[6] G. J. Kramer,[1] R. J. Jayakumar,[6] R. J. La Haye,[3] G. R. McKee,[5] M. A. Makowski,[6] W. A. Peebles,[4] T. L. Rhodes,[4] W. M. Solomon,[1] E. J. Strait,[3] M. A. VanZeeland,[7] and L. Zeng[4]

[1]*Princeton Plasma Physics Laboratory, P.O. Box 451, Princeton, New Jersey 08543, USA*
[2]*University of Texas at Austin, Austin, Texas 78712, USA*
[3]*General Atomics, San Diego, California 92186-5608, USA*
[4]*University of California at Los Angeles, Los Angeles, California 90095, USA*
[5]*University of Wisconsin–Madison, Madison, Wisconsin 53706, USA*
[6]*Lawrence Livermore National Laboratory, Livermore, California 94550, USA*
[7]*Oak Ridge Institute for Science Education, Oak Ridge, Tennessee 37831, USA*

(Received 22 December 2005; published 15 March 2006)

Evidence is presented for a multitude of discrete frequency Alfvén waves in the core of magnetically confined high-temperature fusion plasmas. Multiple diagnostic instruments confirm wave excitation over a wide spatial range from the device size at the longest wavelengths down to the thermal ion Larmor radius. At the shortest scales, the poloidal wavelengths are comparable to the scale length of electrostatic drift wave turbulence. Theoretical analysis confirms a dominant interaction of the modes with particles in the thermal ion distribution traveling well below the Alfvén velocity.

DOI: 10.1103/PhysRevLett.96.105006 PACS numbers: 52.35.Bj, 52.55.Fa, 52.55.Pi, 52.35.Kt

Shear Alfvén waves are ubiquitous in astrophysical and laboratory plasmas, and their behavior is of vital importance for the achievement of viable fusion energy in magnetic confinement systems such as ITER [1]. In astrophysics, the cascade of shear Alfvén waves down to the scale of the ion Larmor radius is considered important for understanding wave dissipation and absorption of energy in magnetized accretion flows [2], in the anomalous heating of the solar corona [3], and in the transfer of particles and energy from the solar wind to the magnetosphere [4]. In fusion plasmas, the excitation of very large scale shear Alfvén waves [such as the toroidal Alfvén eigenmode (TAE)] [5,6] is important for addressing the resonant transport of fusion products across magnetic field lines. In contrast, Alfvén waves on the scale of the ion Larmor radius [7] have not received significant attention in fusion experiments, principally due to the long-standing difficulty of performing precision high resolution measurements deep in the interior of these devices. However, recent advances in remote detection techniques have revealed new details on the fine scale properties of these high-temperature plasmas [8–10]. In this Letter, we present new evidence from the DIII-D device [11] for a multitude of discrete shear Alfvén waves in the plasma core where the waves extend in scale from the system size down to orbit width of the thermal ions. Calculations reveal a dominant drive from the ion temperature profile for these short scale modes.

Figure 1 displays the evolution of basic plasma parameters together with the spectrogram of core density and edge magnetic oscillations in a quiescent double barrier (QDB) discharge on DIII-D [12]. An important property of QDB plasmas, relevant to the present study, is the presence of large ion temperature gradients in the region of reduced magnetic shear in the plasma core. Magnetic fluctuations are measured using external coils. Density fluctuations are measured using far infrared (FIR) scattering of 300 GHz electromagnetic waves. QDB plasmas are heated using 80 keV deuterium neutral beams injected into the plasma in the direction opposite to the plasma current. The neutral beam ion velocity (V_b) and the thermal ion velocity (V_i) are well below the Alfvén velocity (V_A) in this discharge [Fig. 1(b)]. The spectrogram of magnetic fluctuations [Fig. 1(d)] shows no sign of the high frequency oscillations that are present on the FIR scattering signals [Fig. 1(e)]. The peak density fluctuation intensity is 6 orders of magnitude above background with no discernible signature on the magnetic coils.

Figure 2(a) displays a broader spectral and temporal range of the same FIR signal shown in Fig. 1(e). The spectrum is characterized by multiple bands of modes with mean frequency increasing steadily in time. Each band is actually made up of many discrete modes chirping down in frequency and decaying as the next mode appears. A simplified model of reverse shear Alfvén eigenmodes (RSAEs) [13] (also called Alfven cascades) reproduces the spectral evolution of the core-localized modes as shown in Fig. 2(b). The RSAE is a shear Alfvén wave localized to the magnetic shear reversal point where the safety factor is at its minimum value $q_{\min}$. For toroidal mode number n and poloidal mode number m, a shear Alfvén wave (or RSAE) propagates along magnetic field lines with a frequency given by $\Omega_{m,n} \simeq k_{\|}^{m,n} V_A$, where $k_{\|}^{m,n} = (m - nq)/qR$. The RSAE frequency is expected to sweep from low values to the TAE frequency ($\Omega_{\mathrm{TAE}} = V_A/2qR$) as $q_{\min}$ decreases between the values m/n and $(m - 1/2)/n$. The magnetic safety factor q is determined from motional Stark effect (MSE) spectroscopic measurements [14]. The measured

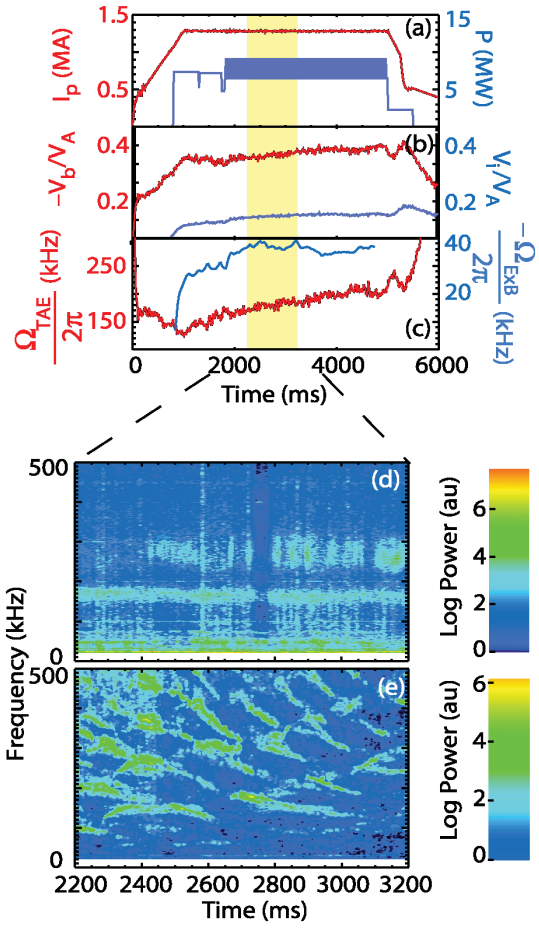

FIG. 1 (color). Evolution of plasma parameters in a QDB plasma (no. 107001) with toroidal magnetic field $B_T = 2.05$ Tesla: (a) plasma current (I_p) and deuterium neutral beam power (P), (b) ratio of neutral beam velocity (V_b) and thermal ion velocity (V_i) to the Alfvén velocity (V_A), (c) TAE frequency ($\Omega_{\mathrm{TAE}}/2\pi$) and $E \times B$ induced Doppler shift for an $n = 1$ mode ($\Omega_{E\times B}/2\pi$), (d) magnetic fluctuation spectra measured outside of the plasma boundary, and (e) density fluctuation spectra in the plasma core measured using FIR scattering. Local parameters are major radius $R = 1.94$ m corresponding to the location of $q = q_{\min}$, ion temperature $T_i = 11$ keV, electron temperature $T_e = 4$ keV, and electron density $n_e = 3.5 \times 10^{19}$ cm^{-3}.

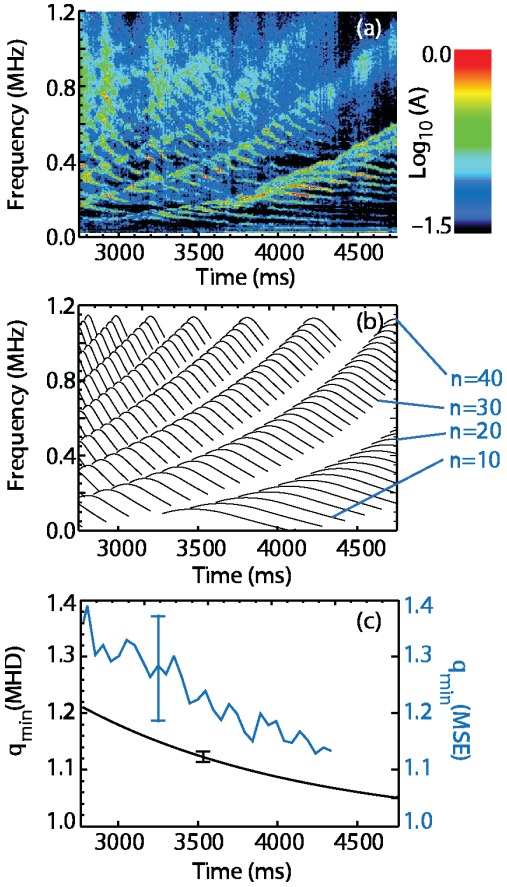

FIG. 2 (color). (a) Evolution of FIR scattering spectrum, (b) model analysis of frequency evolution of RSAEs at $q_{\min}$ indicating toroidal mode numbers in the range $n = 8$–40, and (c) comparison of model prediction to MSE measurement of the evolution of $q_{\min}$ over the measurement interval.

evolution of $q_{\min}$ is shown in Fig. 2(c). In addition, V_A is calculated from the measured electron density profile using spatially resolved high-k laser scattering.

The observed frequencies in Fig. 2(a) far exceed the characteristic TAE frequency [Fig. 1(c)]. However, a radial electric field can also induce a Doppler shift in the laboratory frame given by $\Omega_{\mathrm{Dop}} = n\Omega_{E\times B}$, where $\Omega_{E\times B} = E_r/RB_\theta$, E_r is the radial component of the electric field and B_θ is the poloidal magnetic field strength [15,16]. An additional frequency shift is also expected due to the ion diamagnetic drift flow of the plasma [7], which is proportional to the ion pressure gradient and is given by $\omega^*_{pi} = -qn(dT_i n_i/dr)/m_i\omega_{ci} r n_i$, where the ion pressure is $n_i T_i$, with n_i the ion density, m_i the ion mass, T_i the ion temperature, and ω_{ci} the ion cyclotron frequency. Incorporating diamagnetic flows, the predicted frequency in the $E_r = 0$ frame becomes

$$\hat{\Omega}_{m,n} = \pm[\Omega^2_{m,n} + \omega^{*2}_{pi}/4]^{1/2} + \omega^*_{pi}/2, \qquad (1)$$

where $\Omega_{m,n}$ is the eigenfrequency predicted within ideal MHD theory. We choose the sign that make the two terms on the right-hand side of Eq. (1) reinforce each other. In the lab frame, the observed frequencies are given by $\omega_{m,n} = \hat{\Omega}_{m,n} + n\Omega_{E\times B}$.

From Fig. 1(c), $\Omega_{E\times B}$ is near 20% of the TAE frequency and of opposite sign, suggesting very high-n modes must be involved in order to reverse the apparent direction of the frequency sweep of RSAEs and give rise to such high frequency signals in Fig. 2(a). At the radial location of $q_{\min}$, $\Omega_{E\times B}$ is in the range 37–40 kHz from Fig. 1(c); however, for these plasmas, the diamagnetic shift can reduce the frequency difference between successive modes by $\simeq$8 kHz relative to $\Omega_{E\times B}$, leading to an inferred frequency difference in the range 29–35 kHz, close to the average difference of 32 kHz between successive modes in Fig. 2(a).

Figure 2(b) shows the calculated frequency evolution of RSAEs based on plasma parameters measured in the time interval in Fig. 2(a). This analysis uses an effective Doppler shift of 32 kHz in the direction opposite to the plasma current, equivalent to the average frequency separation observed between successive modes in each band [16]. The minimum and maximum mode frequency $\Omega_{m,n}$ are calculated using the ideal MHD code NOVA [17], which takes as input parameters the measured equilibrium profiles of the plasma pressure, toroidal current, and plasma shape. The NOVA code also accounts for the plasma compressibility [18,19] and radial pressure gradient [20], which are essential for the lower frequency behavior of shear Alfvén eigenmodes. The only adjustable parameter in this model is the range of $q_{\min}$ which is chosen to conform closely to the measured values from MSE [Fig. 2(c)] and to reproduce the observed mode frequency evolution in Fig. 2(a). The frequency spectrum of the FIR data is reproduced using Eq. (1) for toroidal mode numbers chosen in the range $n = 8$–40.

Radially and poloidally localized measurements confirm the short scale nature of these modes inferred from FIR scattering data. The local density fluctuations are obtained with a radial and poloidal resolution of $\simeq$1 cm using the beam emission spectroscopy (BES) diagnostic [8]. Figure 3 shows BES measurements taken at the location of $q_{\min}$ indicating the presence of RSAE activity. BES measurements taken just 12 cm outside of this location in similar plasmas indicate no significant Alfvén mode activity. Poloidal wave numbers from BES measurements at $q_{\min}$ are shown in Fig. 3(c) for the first two frequency bands (band 1 and band 2) in Fig. 3(b). The poloidal wave number is measured directly from two point correlations between pairs of BES elements in the locally vertical direction. The measured wave numbers decrease with time similar to the decrease of the mode frequencies in Fig. 3(b). This reduction of the poloidal wave number is consistent with the simple estimate $k_\theta \simeq n q_{\min}/r$, where $n \simeq \omega/\Omega_{E\times B}$ valid for a large Doppler shift. Figure 3(d) displays the k_θ from BES measurements vs the local k_θ obtained from the NOVA code at the known location of the BES measurements. The analysis demonstrates qualitative consistency between the BES measured poloidal wave numbers and the predictions from the NOVA code.

The measured poloidal wave numbers are in the range $0.15 < k_\theta \rho_i < 0.55$, where the thermal ion Larmor radius $\rho_i \simeq 0.7$ cm for $T_i \simeq 12$ keV. For comparison, the typical range of electrostatic drift wave fluctuations in tokamaks corresponds to $0.2 < k_\theta \rho_i < 0.5$ for ion temperature gradient (ITG) turbulence [21], suggesting a role for ITG drive in the excitation of these modes [7].

The stability of the system is assessed using the kinetic NOVA-K code [17,22] (a perturbative kinetic extension of NOVA). NOVA-K calculates the wave-particle interaction using the orbit dynamics of particles in the toroidal magnetic geometry, as well as the appropriate distribution functions of the thermal and neutral beam ions. The neutral beam ion distribution is obtained using an analytic model [23] that accounts for the ionization, slowing down, and scattering of the beam injected particles and the resulting distribution is close to the distribution found from the Monte Carlo calculation used in the TRANSP code [24]. In addition, electron collisional and Landau damping are included. The resulting growth rates are shown in Fig. 4. Figure 4(a) shows the contribution to the mode linear growth rate from the suprathermal beam ions, the total contribution to the growth rate from suprathermal and thermal ions, and the net damping rate from electron collisional and Landau damping for a range of toroidal mode

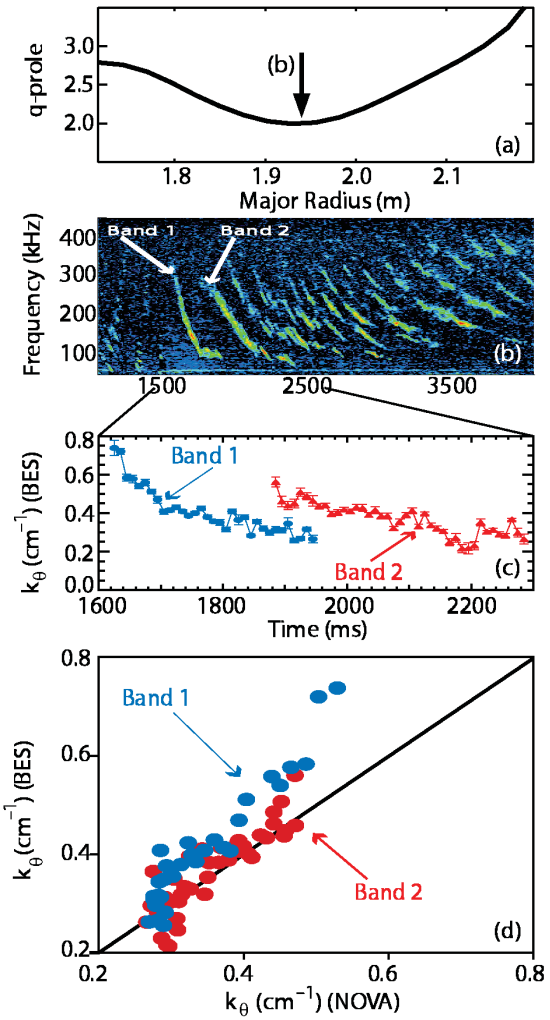

FIG. 3 (color). (a) q profile at 1500 ms in discharge no. 119346, (b) BES spectrum at major radius 1.94 m close to the location of $q_{\min}$ shown in the same color scale used in Fig. 2(a), (c) measured poloidal wave number for the first two frequency bands in (b), and (d) poloidal wave number from BES (vertical) vs the poloidal wave number from the NOVA-K code (horizontal) for the same two frequency bands. Discharge parameters: plasma current 1.0 MA, toroidal magnetic field 2.0 Tesla, central ion temperature 12 keV, central electron temperature 4 keV, and central plasma density 2.0×10^{19} m^{-3}.

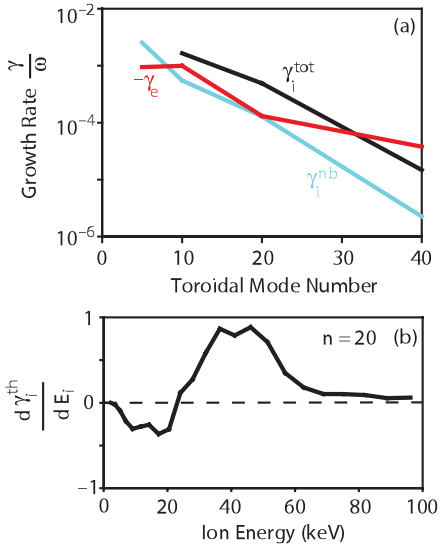

FIG. 4 (color). (a) Linear growth rate normalized to the mode frequency (γ/ω) vs toroidal mode number from the NOVA-K code for discharge no. 107001. Shown are electron collisional and Landau damping ($-\gamma_e$), neutral beam ion drive (γ_i^{nb}), and total ion drive ($\gamma_i^{tot} = \gamma_i^{nb} + \gamma_i^{th}$, where γ_i^{th} is the thermal ion drive). (b) Partial contribution of thermal ions ($d\gamma_i^{th}/dE_i$) to the mode drive vs thermal ion energy for toroidal mode number $n = 20$.

numbers ($n = 5, 10, 20, 40$). The calculation shows that the thermal ions dominate the mode drive for $n \geq 10$ and provide the requisite drive to overcome the electron damping in the range $n \simeq 10$–30. The modes are predicted to be damped for $n = 5$ due to a large thermal ion Landau damping contribution at low n. This range of predicted instability drive is remarkably similar to the range of modes observed in experiment and suggests that the role of thermal ions is critical both to the destabilization of modes at high n and to the suppression of modes at low n. Note that, if we ignore the role of ω_{pi}^* in the thermal ion-mode interaction, then the ion Landau damping exceeds by almost 2 orders of magnitude the beam ion drive for $n > 10$.

Figure 4(b) shows the thermal ion contribution to the mode drive vs the thermal ion energy where γ_i^{th} is the growth rate due to thermal particles and $d\gamma_i^{th}/dE_i$ is the contribution to γ_i^{th} from a fixed energy E_i. These NOVA-K calculations reveal that the dominant resonant interaction is in the range 25–55 keV for a local ion temperature of $\simeq 11$ keV, consistent with the theoretical expectation $E_i/T_i > 5/2$ for Alfvén modes driven by thermal ions. The drive from thermal ions in the Maxwellian tail is a generic property of all temperature gradient driven instabilities, including ITG modes [25] as well as Alfvén modes [7].

In the present work, we have shown the existence of a multitude of short scale shear Alfvén waves in the region of weak magnetic shear in a fusion plasma. The transverse wavelengths can span a wide range of scale from the device size at low n to the thermal ion Larmor radius at high n. Numerical analysis confirms mode excitation over a wide spectral range and indicates a rapid transition to dominant thermal ion drive for $n \geq 10$. The observed range of poloidal wavelengths is similar to that expected for ITG drift wave turbulence in fusion plasmas. A key result of our analysis is that the thermal inhomogeneity of the background plasma strongly modifies the stability of these modes, leading to destabilization by thermal ions traveling well below the Alfvén velocity. This is counter to the conventional wisdom that thermal ions produce net ion Landau damping in reactor grade plasmas and indicates the need to reexamine theoretical predictions of Alfvén mode stability, particularly in advanced reactor regimes where high ion temperature gradients are expected in regions of weak magnetic shear.

This work is supported by the U.S. Department of Energy under DE-AC02-76CH03073, DE-FG03-97ER54415, DE-FC02-04ER54698, DE-FG03-01ER5461, DE-FG03-96ER54373, W-7405-ENG-48, and DE-AC05-76OR00033. The authors thank W. Dorland and T. S. Hahm for helpful discussions.

*Electronic address: rnazikian@pppl.gov

[1] R. Aymar *et al.*, Plasma Phys. Controlled Fusion **44**, 519 (2002).
[2] E. Quataert and G. Gruzinov, Astrophys. J. **520**, 248 (1999).
[3] Y. Voitenko and M. Goossens, Astrophys. J. **605**, L149 (2004).
[4] D. Sundkevist *et al.*, Nature (London) **436**, 825 (2005).
[5] K. L. Wong *et al.*, Phys. Rev. Lett. **66**, 1874 (1991).
[6] W. W. Heidbrink *et al.*, Nucl. Fusion **31**, 1635 (1991).
[7] F. Zonca *et al.*, Plasma Phys. Controlled Fusion **38**, 2011 (1996).
[8] G. McKee *et al.*, Phys. Rev. Lett. **84**, 1922 (2000).
[9] R. Nazikian *et al.*, Phys. Rev. Lett. **94**, 135002 (2005).
[10] S. Sharapov *et al.*, Phys. Rev. Lett. **93**, 165001 (2004).
[11] E. J. Strait *et al.*, Phys. Rev. Lett. **75**, 4421 (1995).
[12] C. M. Greenfield *et al.*, Phys. Rev. Lett. **86**, 4544 (2001).
[13] H. L. Berk *et al.*, Phys. Rev. Lett. **87**, 185002 (2001).
[14] F. M. Levinton *et al.*, Phys. Rev. Lett. **63**, 2060 (1989).
[15] T. S. Hahm and W. M. Tang, Phys. Plasmas **1**, 2099 (1994).
[16] E. J. Strait *et al.*, Plasma Phys. Controlled Fusion **36**, 1211 (1994).
[17] C. Z. Cheng, Phys. Fluids B **3**, 2463 (1991).
[18] A. D. Turnbull *et al.*, Phys. Fluids B **5**, 2546 (1993).
[19] B. N. Breizman *et al.*, Phys. Plasmas **12**, 112506 (2005).
[20] G. J. Kramer *et al.*, Plasma Phys. Controlled Fusion **46**, L23 (2004).
[21] A. M. Dimits *et al.*, Nucl. Fusion **41**, 1725 (2001).
[22] N. N. Gorelenkov *et al.*, Phys. Plasmas **6**, 2802 (1999).
[23] N. N. Gorelenkov *et al.*, Nucl. Fusion **45**, 226 (2005).
[24] R. V. Budny, Nucl. Fusion **42**, 1383 (2002).
[25] B. Coppi *et al.*, Phys. Fluids **10**, 582 (1967).